LOSS MODELING AND COMPONENT SELECTION FOR RESONANT POLE INVERTERS

David Perreault Henrik Martin Robert Selders John Kassakian

Laboratory for Electromagnetic and Electronic Systems
Massachusetts Institute of Technology
Cambridge, MA 02139 U.S.A.

ABSTRACT

This paper addresses the design of resonant pole inverter cells at the pc-board level, including loss modeling and resonant component selection. Tradeoffs between operating frequency, minimum switching current, inductor energy storage, and converter losses are described for selecting resonant components. Two methods are presented for estimating converter losses as a function of resonant components and operating point. The first method uses closed-form equations based on very simple device models, while the second is based on simulation of the converter over one switching cycle using more complex device models.

INTRODUCTION

The construction of high-power converter systems using a cellular architecture, in which large numbers of low-power converter cells are paralleled to achieve a high power rating, has been the focus of recent research [1-3]. The cellular architecture has several potential advantages over conventional design approaches, including improved performance, higher reliability, and reduced cost [1],[2]. The Resonant Pole Inverter (RPI) is one promising topology for low-power converter cells at the pc-board level. This topology, shown in the half-bridge configuration in Fig. 1, has many advantages including simplicity, small output magnetics, and the ability to operate at high frequencies.

To take advantage of the Resonant Pole topology, design methodologies for the RPI cells must be developed. This paper addresses the design of RPI cells including the selection of resonant components and modeling of converter losses. A method for selecting the resonant components in Resonant Pole Inverters has been presented in [4], but this approach does not provide a full view of the tradeoffs in sizing the resonant components. Tradeoffs between operating frequency, minimum switching current, inductor energy storage and converter losses will be elucidated. Two methods will be presented for obtaining converter loss estimates as a function of resonant components and the operating point. The first method uses closed form equations based on very simple device models, while the second is based on simulation of the converter with more complex device models.

CALCULATING RPI POWER LOSSES

In order to design Resonant Pole Inverter cells, it is important to be able to predict converter losses as a function of resonant components and operating point. While crude predictions of device losses usually suffice for resonant component selection, more exact models are desirable for validating these predictions and designing the thermal management system. Two methods of obtaining these estimates are presented here. The first method uses closed-form equations based on very simple models of the devices. This method allows rapid calculation of the loss surface (over varying resonant component values) at the expense of accuracy. The second method is based on simulation of the converter over one switching cycle using more complex device models. This provides a better picture of the loss surface at large computational expense.

With either estimation method, the approach for obtaining a loss surface is the same. First, a range is picked to evaluate C_r and L_r over. One possible guideline is to pick $C_{r,max}$ to be below the range where it provides significant clamping on the device during turn-off, and to pick $L_{r,max}$ such that the switching frequency never falls below some desired value at full load. For a given L_r and C_r, the losses in a switching cycle are a function of output voltage and peak commanded current in the converter. For a given output voltage, losses should always be evaluated at the peak possible commanded current to obtain the worst-case condition. The power loss is evaluated over the range of output voltage, and the maximum loss is retained as the worst case for that set of resonant components. Once the parameter range of L_r and C_r is covered, the data can be plotted and used in the component optimization process.

Closed-Form Loss Calculations

At constant load, the total device losses in the RPI can be modeled as:

$$P = f[E_{cond}(i_{p+}, i_{p-}) + E_{off}(i_{p+}) + E_{off}(i_{p-}) + 2E_{on}] \quad (1)$$

where f is the switching frequency at the operating point, E_{cond} is the conduction loss over one cycle, E_{off} is the turn-off loss at the specified current, and E_{on} is the turn-on loss for the device. The peak currents (i_{p+}, i_{p-}) used are dictated by the RPI control strategy. For all such strategies, the peak currents are specified as a function of the reference current, filter capacitor voltage, and circuit parameters [4,5].

The switching frequency of the RPI varies with operating point. If the resonant transitions are short, and do not strongly affect the resonant inductor current, the operating frequency of the converter can be approximated as:

$$f = \frac{\frac{1}{4}V_{dc}^2 - V_{cf}^2}{V_{dc}L_r(i_{p+} + i_{p-})}. \quad (2)$$

It should be noted that this expression is based on a triangular approximation of the inductor current waveform (Fig. 1), and becomes less accurate when the inductor current waveform becomes significantly nontriangular due to the resonant transitions.

The device model used for closed-form loss calculations assumes constant forward and reverse conduction voltage drops of V_{cf} and V_{dr}. Using this model allows the conduction loss energy in a device to be approximated as the device drop times the appropriate area under the inductor current waveform. Using the triangular approximation to the inductor current, this model predicts a per-cycle conduction loss for all devices in a half-bridge of:

$$E_{cond} = \frac{L_r}{2(\frac{1}{4}V_{dc}^2 - V_{cf}^2)} \cdot [\tfrac{1}{2}V_{dc}(V_{cf} + V_{dr})(i_{p+}^2 + i_{p-}^2) + V_{cf}(V_{cf} - V_{dr})(i_{p+}^2 - i_{p-}^2)] \quad (3)$$

For closed-form calculations, a linear-fall turn-off model is used with current fall time t_f. This model is simple, but often adequate for selecting resonant components [6]. It is assumed that the inductor current change during device turn-off is negligible, leading

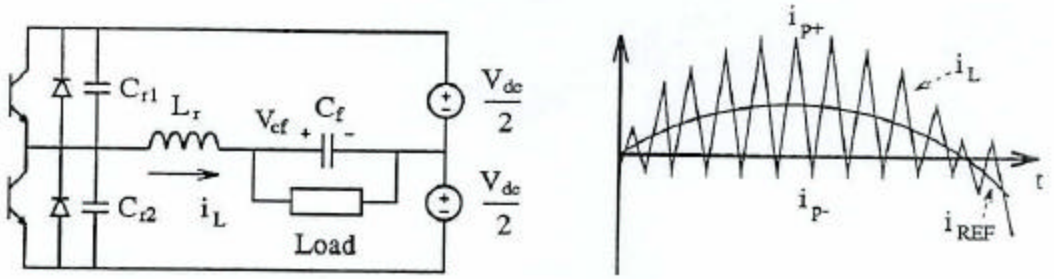

Figure 1 The Resonant Pole Inverter and its output current waveform.

to the turn-off model of Fig. 2. For turning off currents I_o such that:

$$I_o \le \frac{4 V_{dc} C_r}{t_f} \qquad (4)$$

the device will be well snubbed, and turn off before the voltage across it rises to the full bus voltage. In this case the turn-off loss for the switch under this model is:

$$E_{off} = \frac{I_o^2 t_f^2}{48 C_r} . \qquad (5)$$

For currents higher than specified in (4), the turn-off loss under this model becomes:

$$E_{off} = \frac{1}{2} V_{dc} I_o t_f + V_{dc}^2 C_r - \frac{4}{3} V_{dc} \sqrt{V_{dc} I_o C_r t_f} \qquad (6)$$

Note that these calculations do not include dissipation of device package leakage inductance energy, which must be handled separately if it is a significant component.

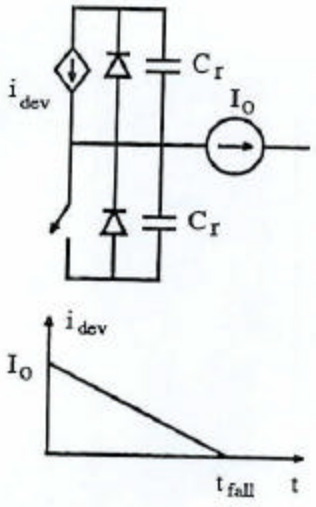

Figure 2 The device turn-off model used in closed-form calculations.

Ideally, the Resonant Pole Inverter has no turn-on loss, since the incoming device turns on while its antiparallel diode is conducting. However, some power devices such as MCTs [6] and IGBTs [7-8] exhibit a transient voltage spike at turn-on. These effects depend on the device manufacture, and vary significantly among different types of devices. To model this effect, it is assumed that the device does not turn on until a certain voltage V_{on} is built up across it. Once this voltage is reached, the device turns on and its voltage drops to V_{dr}. The energy stored in the resonant capacitors during the voltage build up is dumped into the device when it turns on. Assuming that V_{on}^2 is much larger than V_{dr}^2, the energy loss during turn on of a switch is then approximately:

$$E_{on} = C_r V_{on}^2 . \qquad (7)$$

Combining these loss terms as specified in (1) yields an analytical calculation of the expected power dissipation for a given operating point, and can easily be used to calculate the loss surface as previously described. These equations represent a significant extension of the loss calculations made in [4], and bear little relation to the method used in [9], which assumes a 50% duty cycle and entirely ignores switching losses.

Simulation-Based Loss Calculations

Use of closed-form loss calculations allows rapid computation of an approximation to the loss surface. However, more accurate methods are often desirable, such as when making final component selections or designing the thermal management system. Limitations of the closed-form method include the inaccuracy of the turn-off and conduction loss models for many devices, and the limited accuracy of (2) under some conditions. For these reasons, loss calculations based on a simulation approach have also been developed. To calculate losses, the circuit is simulated for one switching cycle at the specified operating point, with the output voltage assumed clamped at the specified point by the output filter. Turn-off losses are predicted using a linear-and-tail turn-off model (Fig. 3), which is simple while accurately capturing the behavior of many real devices. Conduction losses are calculated using constant plus resistive drop models for both forward (V_{df}, R_{df}) and reverse (V_{dr}, R_{dr}) conduction. The method also allows addition of other effects, such as resonant capacitor nonlinearities, inductor ESR, etc., but these effects will be excluded here for simplicity.

State equations for the converter of Fig. 1 are required for each possible switch state along with conditions for transitioning to the next switch state, allowing simulation for the converter for an operating cycle. Equations to calculate the power loss in each device pair (S_1/D_1, S_2/D_2) over a time step are also needed for each possible switch state. Simulation of the converter over a full cycle while adding up the losses at each time step yields the total energy loss over a cycle. Note that the relevant state variables are the resonant inductor current and either of the resonant capacitor

voltages. For simplicity, the device drops on the capacitor voltages are ignored when finding the transition points between switch states. During turn off, the device current is calculated as shown in Fig. 3, where t is the time referenced to the beginning of turn off. For brevity, state and power loss equations are only provided for one half of the operational cycle, since the equations for the other half of the cycle are very similar. The simulation equations are as follows:

State A: S_1 on D_1, S_2, D_2 off:

$$\frac{di_L}{dt} = \frac{1}{L_r}\left[\frac{1}{2}V_{dc} - V_{cf} - V_{df} - i_L R_{df}\right] \qquad (8)$$
$$\frac{dV_{c1}}{dt} = 0$$

$$\Delta E_1 = i_L(V_{df} + R_{df} i_L)\Delta t \qquad (9)$$
$$\Delta E_2 = 0$$

This state lasts until $i_L > i_{rr}$. At this point, S_1 is turned off, causing a transition to state B.

State B: S_1 turning off or off, D_1, S_2, D_2 off:

$$\frac{di_L}{dt} = \frac{1}{L_r}\left[\frac{1}{2}V_{dc} - V_{cf} - V_{c1}\right] \qquad (10)$$
$$\frac{dV_{c1}}{dt} = \frac{1}{2C_r}\left[i_L - i_{dev}\right]$$

$$\Delta E_1 = i_{dev} V_{c1}\Delta t \qquad (11)$$
$$\Delta E_2 = 0$$

This state lasts until $V_{c1} < 0$, when state C is entered.

State C: S_1 turning off or off, D_2 on, D_1, S_2 off:

$$\frac{di_L}{dt} = -\frac{1}{L_r}\left[\frac{1}{2}V_{dc} + V_{cf} + V_{df} + (i_L - i_{dev})R_{df}\right] \qquad (12)$$
$$\frac{dV_{c1}}{dt} = 0$$

$$\Delta E_1 = i_{dev} V_{c1}\Delta t \qquad (13)$$
$$\Delta E_2 = (i_L - i_{dev})\left[V_{df} + (i_L - i_{dev})R_{df}\right]\Delta t$$

This state lasts until $i_L < 0$. If turn-on transient effects are considered, state Y is entered. Otherwise, state D is entered directly.

State Y: S_1, D_1, D_2 off, S_2 turning on:

$$\frac{di_L}{dt} = \frac{1}{L_r}\left[\frac{1}{2}V_{dc} - V_{c1} - V_{cf}\right] \qquad (14)$$
$$\frac{dV_{c1}}{dt} = \frac{i_L}{2C_r}$$

$$\Delta E_1 = 0 \qquad (15)$$
$$\Delta E_2 = \frac{1}{2}(V_{c1} + V_{c2})i_L\Delta t$$

This state only occurs when modeling the turn-on transient of S_2. Loss energy is calculated as the incremental energy which is stored on the resonant capacitors, and is dissipated instantaneously when S_2 triggers on. This state ends when $V_{c2} > V_m$. At this point, S_2 triggers on, V_{c2} is reset to 0, V_{c1} is reset to V_{dc}, and state D is entered.

The state and power loss equations for the second half of the converter operating cycle are similar to those of the first half, and are omitted for brevity. The states the converter traverses in the second half of the cycle are:

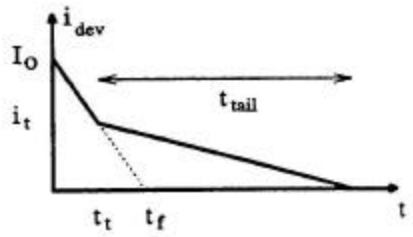

Figure 3 The linear-and-tail turn-off model.

State D: S_2 on, S_1, D_1, D_2 off
State E: S_2 turning off or off, S_1, D_1, D_2 off
State F: S_2 turning off or off, D_1 on, S_1, D_2 off
State Z: S_1 turning on, D_1, S_2, D_2 off

This simulation approach yields a more accurate picture of the losses at a given operating point at significant computational expense compared to the closed-form equations. It also provides a more accurate picture of the operating frequency as a function of operating point than (2), especially when the inductor current waveform is significantly affected by the resonant transitions.

SIZING RESONANT ELEMENTS

Sizing the resonant elements is a complex but critical component of RPI cell design. One method for selecting the resonant components in Resonant Pole Inverters was presented in [4]. This approach is based on minimizing converter losses for a prespecified operating condition and switching frequency. While this approach has merit, it does not provide a full view of the tradeoffs in sizing the resonant components of the RPI cells in a cellular architecture.

Sizing the resonant elements in an RPI cell involves trading between several competing factors, including total power dissipation, minimum switching current, inductor energy storage, full-load minimum switching frequency, and no-load maximum switching frequency.

Power dissipation is an important aspect of the component selection process. Given estimates of the loss surfaces for different device parameters, selection of the best available semiconductor devices can be made. For the main devices, one generally has to trade off between forward drop, turn-off fall time, and turn-on voltage transient losses. The loss surface over the range of resonant component values also allows the designer to restrict attention to component values which are practical from thermal design considerations, and to trade-off thermal management requirements with other design objectives.

In addition to addressing peak power dissipation, it is important to address what happens at partial load when selecting resonant components. The partial-load performance of the RPI cell is strongly affected by the minimum peak switching current which is required to maintain zero voltage switching. This minimum current is in turn a function of the resonant component values. As described in [3,5], the minimum peak current which must be maintained for zero-voltage switching is:

$$i_{min} = 2\sqrt{\frac{C_r}{L_r}V_{dc}\,|V_{cf}|}\,. \qquad (16)$$

Keeping this current small relative to the current rating of the co is important for achieving a design with good partial lo performance.

The energy storage requirement of the resonant inductor is anoth important aspect of RPI cell design. As discussed in [2-3], the si

and cost of the output magnetics in a cellular architecture can be significant. It is thus important to address the resonant inductor sizing as part of the design process. Calculating the energy storage of the resonant inductor as:

$$W_r = \frac{1}{2} L_r i_p^2 |_{max} \qquad (17)$$

it can be seen that the energy storage is a function of both resonant component values, since i_p is partially determined by (16).

The final major considerations when selecting the resonant components are the maximum and minimum switching frequencies that occur over the load range of the cell. The minimum switching frequency of the RPI occurs at full load (max I_{out}, V_{in}), and is a function of the specified voltage bus utilization (80-90% typical) as can be seen in (2). The minimum switching frequency is important because it impacts the spectral performance of the cell and the resulting output filter design. The maximum switching frequency occurs at no load (min I_{out}, V_{in}), and is important mainly because it determines the required bandwidth of the sensing and control circuitry of the RPI cell. Because significant time may be spent in the resonant transitions at no load, it is best to verify maximum switching frequencies using simulation, instead of relying on (2).

Selecting resonant component values is thus a multi-attribute trade-off between the conflicting goals of minimum power dissipation, minimum switching current, minimum magnetic energy storage, and desired switching frequency range. By examining each of these aspects as a function of resonant component values, the designer can select the devices and resonant components which yield the best possible combination of attributes for the application.

CONCLUSION

The resonant pole inverter is a promising topology for the cells in a cellular converter architecture. This paper has addressed the loss modeling and the selection of devices and resonant components in the design of low-power RPI cells. Two methods for estimating the loss surface over resonant components have been presented. The first is based on closed-form expressions, and is very computationally efficient. The second is based on simulation, and yields more accurate results at the expense of computational overhead. The multi-attribute trade-off in selecting resonant component values has also been described, and a design methodology suggested.

ACKNOWLEDGEMENTS

The authors gratefully acknowledge the support provided for this work by the Bose Foundation and the American Power Conversion Corporation.

REFERENCES

[1] Kassakian, J.G. : "High Frequency Switching and Distributed Conversion in Power Electronic Systems", Sixth Conference on Power Electronics and Motion Control (PEMC 90, Budapest), 1990.

[2] Kassakian, J.G. and Perreault, D.J. : "An Assessment of Cellular Architectures for Large Converter Systems", First International Conference on Power Electronics and Motion Control (IPEMC 94, Beijing), June 1994 (in press).

[3] Perreault, D.J., Kassakian, J.G. and Martin, H. : "A Soft-Switched Parallel Inverter Architecture with Minimal Output Magnetics", 1994 IEEE Power Electronics Specialists Conference (PESC 94, Taipei), June 1994 (in press).

[4] Divan, D., Venkataramanan, G., and DeDoncker, R. : "Design Methodologies for Soft-Switched Inverters", IEEE Transactions on Industry Applications, Jan/Feb 1993, pp. 126-135.

[5] Divan, D. and Skibinski, G. : "Zero Switching Loss Inverters for High Power Applications", IEEE IAS Annual Meeting, 1987, pp. 627-634.

[6] DeDoncker, R., Jahns, T., Radun, A., Watrous D. and Temple, V. : "Characteristics of MOS-Controlled Thyristors under Zero Voltage Soft-Switching Conditions", IEEE Transactions on Industry Applications, Vol. 28 No. 2, Mar/Apr 1992, pp. 387-394.

[7] Kurnia, A., Stielau, O., Venkataramanan, G., Divan, D. : "Loss Mechanisms in IGBTs Under Zero Voltage Switching", 1992 IEEE Power Electronics Specialists Conference (PESC 92, Seville), June 1992, pp. 1011-1017.

[8] Consoli, A., Licitra, C., Musumeci, S., Testa, A., Frisina, F. and Letor, R. : "On the Selection of IGBT devices in Soft-Switching Applications", 1993 European Power Electronics Conference (EPE 93, Brighton), Sept. 1993, Vol. 2, pp. 337-343.

[9] Ferreira, J., and van Wyk, J. : "Component Loss Modeling in Hard Switched and Resonant Pole Inverters", IEEE IAS Annual Meeting, 1991, pp. 1462-1467.